LWT - Food Science and Technology 140 (2021) 110695

Contents lists available at ScienceDirect

LWT

journal homepage: www.elsevier.com/locate/lwt

Influence of the wall material on the moisture sorption properties and conditions of stability of sesame oil hydrogel beads by ionic gelation

S.K. Velázquez-Gutiérrez [a], E. Alpizar-Reyes [a], A.Y. Guadarrama-Lezama [a], J.G. Báez-González [b], J. Alvarez-Ramírez [c], C. Pérez-Alonso [a,*]

[a] Facultad de Quimica, Universidad Autonoma del Estado de Mexico, Paseo Colon esq. Paseo Tollocan s/n, Col. Residencial Colon, Toluca, Estado de Mexico, C.P. 50120, Mexico
[b] Departamento de Alimentos, Facultad de Ciencias Biologicas, Universidad Autonoma de Nuevo Leon, Av. Universidad s/n, Cd. Universitaria, Monterrey, Nuevo Leon, C. P. 66455, Mexico
[c] Departamento de Ingenieria de Procesos e Hidraulica, Universidad Autonoma Metropolitana-Iztapalapa, San Rafael Atlixco No. 186, Col. Vicentina, Mexico City, C.P. 09340, Mexico

ARTICLE INFO

Keywords:
Sodium alginate
Nopal mucilage
Hydrogel beads
Ionic gelation
Minimum integral entropy

ABSTRACT

Sesame oil was encapsulated by ionic gelation using matrices of sodium alginate and nopal mucilage as wall material. Moisture sorption isotherms of three different types of hydrogels beads formed by SA-NM (1:0 w/w), SA-NM (1:1 w/w) and SA-NM (1:1.5 w/w) were performed at 25, 35 and 45 °C. Experimental isotherms were described by means of the GAB model, showing sigmoidal shape. Pore radius values of beads ranged from 0.81 to 7.59 nm, corresponding to micropores and mesopores classification. The integral thermodynamic properties were estimated to define conditions of maximum stability of the hydrogel beads. The point of maximum stability, linked to minimum integral entropy, was in the range 3.31–5.59 kg H_2O/100 kg d.s. (corresponding to water activity, a_W, of 0.23–0.59) in the studied temperature range. Enthalpy-entropy compensation for the beads exhibited the presence of two isokinetic temperatures; one at low moisture contents (0–5.95 kg H_2O/100 kg d.s.) controlled by variations of the water entropy, and a second given by enthalpy-driven mechanisms. Overall, the results showed that the hydrogel beads exhibited features of micro- and meso-porous biomaterials. Besides, the composition of the wall material has central implications for the characteristics of the sorption process.

1. Introduction

Sesame oil (*Sesamum indicum* L.) contains high essential fatty acids (ω-3e6), tocopherols, sterols and tocotrienols (Corso et al., 2010). These components of sesame oil improve digestive system and lower blood cholesterol levels (Mudgil & Barak, 2013; Paddon-Jones et al., 2015; Xu-Yan et al., 2012). The industrialization of sesame oil allows its application for food, pharmaceutical and cosmetic industries (Brigante et al., 2020). However, unsaturated essential fatty acids contained in sesame oil exhibit chemical instability in the face of environment stress (e.g., light, oxygen, and moisture). The oxidation of sesame oil not only decreases their nutritional value, but also might result in the generation of toxic products as well as off-flavor and taste. In this regard, encapsulation of sesame oil can be used for protection against environment adverse effects and to allow easier handling, processing, and storage (Alpizar-Reyes et al., 2020; Shahidi & Zhong, 2005).

The ionic gelation process is a relatively simple approach for the encapsulation and stabilization of chemically unstable oil, as well as for the control of oxidative reaction and delivery of active compounds. Besides, ionic gelation is a useful tool for masking flavors, colors and odors, which in turn leads to extended shelf life and protection of active components under environmental factors (Bannikova et al., 2018; Menin et al., 2018). Ionic gelation results in the formation of a hydrogel bead with the bioactive trapped inside. The nature of the hydrogel matrix or wall material surrounding the bioactive can be designed to improve its physical and chemical stability, as well as to control its delivery. It has been reported that the internal structure of beads formed only with sodium alginate as wall material in the encapsulation of oils is extremely porous, with relatively large pore sizes (Bannikova et al., 2018; Menin et al., 2018). On the other hand, nopal mucilage is a biomaterial with extensive applications as food thickener and emulsifier, as well as water retainer and encapsulating medium for bioactive compounds

* Corresponding author.
E-mail address: cpereza@uaemex.mx (C. Pérez-Alonso).

https://doi.org/10.1016/j.lwt.2020.110695
Received 29 September 2020; Received in revised form 30 November 2020; Accepted 1 December 2020
Available online 4 December 2020

(León-Martínez et al., 2010; Medina-Torres et al., 2013). In combination with diverse biopolymers, including κ-carrageenan, nopal mucilage has shown to improve gel rigidity as compared to single materials (Medina-Torres et al., 2013). Also, mixtures of nopal mucilage and sorghum starch showed improvements of gel structure and stability (Rivera-Corona et al., 2014).

The general stability of food matrices is strongly dependent on environment conditions, including moisture content, temperature and water activity (Cano-Higuita et al., 2015; Esquerdo et al., 2019; Monte et al., 2018). Tests based on water vapor adsorption isotherm are commonly used to assess the water activity in food products. Sorption isotherms are useful to assess shelf-life stability and structural characteristics, such as specific surface area, thermodynamic properties, crystallinity and porous structure (Ciurzyńska et al., 2019). In particular, an accurate characterization of the pore structure is a central step to assess the potential mechanisms governing mass transfer processes. These characterization techniques are based on measurements of pore size (e.g., the Kelvin equation) (Alpizar-Reyes et al., 2017; Singh et al., 2006).

Sorption isotherms are important experimental analyzes to estimate valuable thermodynamic properties and to estimate the water content, water activity and temperature for which a dried food product exhibits maximal shelf stability (Escalona-García et al., 2016; Fan et al., 2019). For instance, the minimum integral entropy is a parameter referring to the conditions of maximum stability as linked to strong adsorbate-adsorbent bonds. Under such conditions, free water is more constrained to act in spoilage reactions (Nunes & Rotstein, 1991). On the other hand, energetic and ordering (i.e., enthalpic and entropic) mechanisms and pore-water interactions commonly exhibit positive correlations, providing in this way a suitable framework to address hydrophobic and hydrophilic interactions between water and diverse biomolecules (Labuza et al., 1985; Pérez-Alonso et al., 2006; Rodríguez-Bernal et al., 2015). In general, the accurate characterization of the thermodynamical properties of dried hydrogel beads would provide interesting insights on shelf stability under water activity.

This work focused on the characterization of sodium alginate-nopal mucilage blends as wall material for encapsulation of sesame oil. The main hypothesis is that the relative sodium alginate-nopal mucilage fractions have a determinant role on the moisture sorption properties and the stability conditions of sesame oil hydrogel beads obtained by ionic gelation. In this way, the aim of this work was to establish conditions (e.g., water content, water activity and temperature) for stable shelf life by means of the estimation of the minimum integral entropy of water vapor molecules adsorbed on hydrogel bead surface. A further aim is to determine sorption properties and driving mechanisms of water vapor adsorption on hydrogel beads.

2. Materials and methods

2.1. Materials

The sesame seeds and the nopal (*Opuntia ficus indica)* cladodes were purchased from a market (Toluca, Mexico). Thorns were eliminated from nopal cladodes. The composition of the nopal is very variable, since it depends on species, growing area and growing season. Due to its adaptive characteristics to arid environments, nopal, regardless of gender, presents high levels of non-structural carbohydrates and mineral matter (P, N, K, Ca, Mg), and low levels of dry matter and crude protein (Santiago-Lorenzo et al., 2016). On the other hand, nopal mucilage from *Opuntia ficus indica* (a member of the *cactaceae* family) is a mixture of acidic and neutral polysaccharides consisting of 24.6–42 g/100 g of arabinose; 21–40.1 g/100 g of galactose; 8–12.7 g/100 g of galacturonic acid; 7–13.1 g/100 g of rhamnose, and 22–22.2 g/100 g of xylose, besides of glycoproteins (Sáenz et al., 2004). It has been reported that nopal mucilage has a molecular weight of 2.3×10^4 to 4.3×10^6 Da and it behaves as a polyelectrolyte (Medina-Torres et al., 2000). Proximal analysis of NM powder reveals it contains carbohydrates (66.65 ± 0.61 g/100 g), protein (6.34 ± 0.61 g/100 g), ashes (23.19 ± 0.69 g/100 g), lipids (0.59 ± 0 g/100 g), and moisture (3.23 ± 0.39 g/100 g) (Rivera-Corona et al., 2014).

Commercial sodium alginate (SA) (Protanal® RF 6650 Alginate) was kindly supplied by FMC Health & Nutrition (Mexico City, Mexico). According with supplier, this biopolymer has purity of 90 g/100 g, high molar mass, high content of guluronic acid (65 g/100 g) and viscosity of between 400 and 600 mPas in 1 g/100 mL solution at 20 °C. All reagents used in analyses were of analytical grade (Sigma Aldrich S.A. de C·V., Toluca, Mexico). Deionized water was used for all experimental runs.

2.2. Sesame oil (SO) extraction

The sesame seeds were cold pressed (Tamer hydraulic press, Model PT-20, Shanghai, China) with parameters 40 cm long and 10 cm diameter plunger. The maximum pressure exerted by the piston was about 8.8×10^8 N/m^2 at ~20 °C. Traces of sesame seeds were removed from the extracted oil by means of a cloth filter. Amber bottles were used to store the filtered oil (~5 °C) for subsequent use (Alpizar-Reyes et al., 2020).

2.3. Nopal mucilage (NM) extraction

The method used to extract the nopal mucilage was reported previously (Cortés-Camargo et al., 2018). To this end, cladodes were obtained as small slices (36 cm^2 of contact area and 2 ± 0.2 mm of thickness). The cladodes slices were weighed put in stainless steel containers (3.5 L). Subsequently, deionized water was added (1:2.5 nopal – water ratio) and the mixture was maintained under stirring (86 °C, 2.5 h). After, residuals solids were separated by decantation, filtered by means of a metallic sieve (No. 100), and spread on a tray for air convection drying (65 °C, 4 h) (HCX II model, San-son plus, Mexico). The size of the dried solids was standardized (40 mesh screen, 420 μm).

2.4. Dispersions and hydrogel beads preparation

First, a sodium alginate (SA) biopolymer dispersion was prepared by adding 2% w/v (10 g/L) of sodium alginate powder into deionized water and keep overnight under shaking (20 °C) to guarantee full hydration of biopolymer. The same procedure and proportions were followed to prepare nopal mucilage (NM) stock aqueous dispersion (2% w/v). Then, the stock aqueous dispersions of SA and NM were mixed taking samples in volume proportion of 1:0 v/v while keeping the total dry matter to 10 g/L; resulting in a dry composition of SA-NM (1:0 w/w). Following this steps, two more stock aqueous dispersions were made to prepare solutions (continuous phase) of SA-NM (1:1 w/w) and SA-NM (1:1.5 w/w) in a dry composition. Then, 10 g of sesame oil (disperse phase) were incorporated dropwise into 100 g of biopolymer stock aqueous dispersions (continuous phase) under continuous agitation with an Ultra-Turrax T50 homogenizer (IKA®-Werke Works Inc., Wilmington, NC, USA) at 6400 rpm during 10 min (Rodea-González et al., 2012). Subsequently, a sample of each homogenized dispersion was extracted in a 10 mL syringe attached with a 0.70 mm tip diameter of needle (22 gauge) and dripped into an aqueous solution of 100 mL of calcium chloride (2.5 g/100 mL) contained in a beaker with mechanical stirring to avoid bead agglomeration. The needle tip was set at 30 cm above the surface of the crosslinking solution (20 drops per minute). The gelling solution (SO - SA - NM/$CaCl_2$ solution) was stirred for 60 min at 20 °C to complete gelation and produce beads. The gelling solution was then washed with deionized water and filtered through a 355 μm mesh and subsequently dried in an oven at 50 °C for 24 h. Finally, the hydrogel beads were stored in amber flasks until later use.

2.5. Sorption isotherms

Hydrogels beads were preconditioned on a Petri dish by covering

homogeneously the dish surface. The dish was introduced in a glass desiccators with P_2O_5 as desiccant (~20 °C, 3 weeks) to reduce to the minimum the moisture content obtained when beads exhibited constant weight. The adsorption isotherms of the beads were obtained by a static gravimetric method for temperatures 25, 35 and 45 °C. The runs were carried out by triplicate. The sorption isotherms were described by the GAB (Guggenheim-Anderson-De Boer) model

$$M = \frac{M_0 C K a_w}{(1 - K a_w)(1 - K a_w + C K a_w)} \quad (1)$$

Here, M represents the equilibrium moisture content (kg water/100 kg of dry solid (d.s.)), M_0 becomes the monolayer moisture content (kg water/100 kg d.s.), and a_W denotes the water activity. The parameters C and K are constants introduced to balance the numerical fitting. The model parameters were obtained by least-squares fitting (OriginLab Corp., Northampton, MA, USA). The GAB model is commonly used for the analysis of isotherms in complex systems, as the model has a strong theoretical background as a generalization of the Langmuir and BET models. A key postulate of the GAB model is that the state of adsorbed molecules (water molecules) in the second and additional layers is quite like the one in superior layers, but different from those of the liquid state.

2.6. Sorption properties of sesame oil hydrogel beads

The solid specific surface of sorption can be estimated by the following expression (Cassini et al., 2006; Rosa et al., 2010):

$$S_0 = M_0 \frac{1}{M_w} N_0 A_{H2O} = 3.5 \times 10^3 M_0 \quad (2)$$

where S_0 is the surface area (m^2/g d.s.), M_w is the water molecular weight (18 g/mol), N_0 represents the Avogadro number (6.0×10^{23} molecules/mol) and A_{H_2o} denotes the area of a water molecule (1.06×10^{-19} m^2).

The critical radius (r_c) applies primarily in the condensation region of the isotherm. This can be determined from the Kelvin equation, which provides a correlation between pore diameter and pore condensation pressure, i.e., the smaller the radius, the lower is the a_W value at which pore condensation occurs. In case of real porous materials consisting of pores of different sizes, condensation will occur first in the pores of smaller radii and will progress into the larger pores, at a relative pressure of unity condensation will occur on those surfaces where the radius of curvature is essentially infinite. The critical radius at different water activities was calculated by the following Kelvin expression:

$$r_c = -\frac{2\sigma V_M}{RT \ln(a_W)} \quad (3)$$

where r_c is the critical radius (m), V_M is the molar volume of water (m^3/mol), σ is the surface tension (N/m), R is the universal gas constant (8.314×10^{-3} kJ/mol K), and a_W is the water activity. In a first stance, water adsorb strongly, forming a monolayered structure on the surface. The monolayer is usually reflected in the first part of the sorption isotherm. After the surface is totally covered by a monolayer, further water molecules are weakly attached to form a multi-layered structure. Here, water-water interactions dominate the stability and structure of the multilayer, and they are reflected in the second part of the adsorption layer. The geometry of the adsorbed multilayer affects the stability of food matrices as expressed by water activity. In particular, the thickness t (nm) of the adsorbed water layer was estimated from the Helsey equation (Moraes & Pinto, 2012; Rosa et al., 2010):

$$t = 0.354 \left(\frac{-5}{\ln a_W} \right)^{1/3} \quad (4)$$

The pore radius is a useful parameter to understand the adsorption process (Sonwane & Bhatia, 2000). The pore radius r_p (nm) was computed as the sum of the multilayer thickness and critical radius (Esquerdo et al., 2019; Monte et al., 2018; Moraes & Pinto, 2012; Rosa et al., 2010), namely,

$$r_p = r_c + t \quad (5)$$

2.7. Conditions of stability of sesame oil hydrogel beads

The vapor adsorption isotherms were used to evaluate the physical stability of the sesame oil hydrogel beads. The integral enthalpy is the average energy of the water molecules adsorbed (bound) to the adsorbent (solid) at a particular hydration level (particular moisture content) (Schneider, 1981). On the other hand, the integral entropy provides an index of the stability of the water ensemble adsorbed on a surface. The change in integral enthalpy at constant pressure of diffusion (Φ) was estimated by

$$\left(\frac{\partial \ln a_W}{\partial (1/T)} \right)_{\Phi} = \frac{H_s - H_1}{R} = \frac{(\Delta H_{\text{int}})_T}{R} \quad (6)$$

In this case, H_s corresponds to the integral molar enthalpy of water molecules (kJ/mol), H_l to the constant temperature and pressure partial molar enthalpy (kJ/mol). Finally, $(\Delta H_{\text{int}})_T$ becomes the change in integral enthalpy at a given temperature (kJ/mol). The change in integral entropy is estimated by

$$(\Delta S_{\text{int}})_T = \frac{(\Delta H_{\text{int}})_T}{T} - R \ln a_W \quad (7)$$

where $(\Delta S_{\text{int}})_T$ is the change in the constant temperature integral entropy. Subsequently, the water activity-temperature conditions reflecting the minimum integral entropy were estimated, which corresponds to the region of maximum storage stability (Hoyos-Leyva et al., 2019). Under minimal integral entropy, water is less available for deterioration of sorption systems in storage conditions (Nunes & Rotstein, 1991).

2.8. Compensation theory

A promising theory that has been widely considered to investigate physical and chemical phenomena involved in water sorption is enthalpy-entropy compensation or isokinetic theory. The isokinetic theory is an important tool in recognizing different mechanisms for water sorption under varying conditions, such as drying processes. The theory states, in order to minimize free energy changes due to these phenomena, that: (i) the compensation (by changing ΔH or ΔS) arises from the nature of the interaction between the sorbent (solid) and sorbate (water) causing the reaction and (ii) the relationship between the enthalpy and entropy for a specific reaction is linear (Beristain et al., 1996). The compensation theory is based on the assumption that the enthalpy-entropy relationship is linear (Alpizar-Reyes et al., 2017). Specifically,

$$(\Delta H_{\text{int}})_T = T_B (\Delta S_{\text{int}})_T + \Delta G_B \quad (8)$$

Here, T_B is the isokinetics temperature and corresponds to the temperature at which all reactions takes place at the same rate. Besides, the free energy corresponding to isokinetic temperature, ΔG_B, is considered as a parameter to determine if the water sorption process is taking place spontaneously ($\Delta G_B < 0$) or driven by a given exogeneous mechanism ($\Delta G_B > 0$). An approach to check the compensation theory considers the isokinetic temperature (T_B) contrasted with the harmonic mean temperature (T_{hm}) (Lara et al., 2020). The isokinetic temperature correspond to the value at which enthalpy and entropy contributions are mutually cancelled out, so that all chemical mechanisms exhibit the same activity. On the other hand, the harmonic temperature is given by

$$T_{hm} = \frac{N}{\sum_{i=1}^{N} (1/T)} \quad (9)$$

Fig. 1. Optical microscopy images of external surface and shape of the hydrogel beads and dry beads for (a) SA-NM (1:0); (b) SA-NM (1:1) and (c) SA-NM (1:1.5).

where N is the number of isotherms used in the computations. A linear enthalpy-entropy compensation is found if $T_B \neq T_{hm}$.

2.9. Statistical analysis

Experimental data are presented as means ± standard deviation from triplicate runs for each sample. One-way analysis of variance (ANOVA) and Turkey's test ($p \leq 0.05$) were conducted by means of Minitab software (Minitab Inc., State College, PA, USA). The fitness of the GAB model for sorption isothermal behavior was assessed by the coefficient of determination (R^2) and the mean relative deviation modulus (E) given by

$$E = \frac{100}{n} \sum \frac{|M_i - M_{Ei}|}{M_i} \quad (10)$$

where Mi is the ith moisture content, M_{Ei} is the corresponding estimated moisture content and n is the observations number. An acceptable fit is considered when $E < 5\%$ (Pérez-Alonso et al., 2006).

3. Results and discussion

3.1. Morphology and color

Fig. 1 presents images of the beads for the three different formulations. The upper panel displays the hydrogel beads and the lower panel the dry beads. Typically, beads containing only sodium alginate (SA:NM 1:0) are white with a spherical-like, although irregular, shape. The incorporation of the nopal mucilage added yellow color and deformed the beads to ellipsoidal shapes. The effect was more pronounced with the increase of the nopal mucilage content. Yellow-greenish spectrum of nopal mucilage was attributed to the proteins, with contents as high as 7.2 g/100 g (Sepúlveda et al., 2007).

3.2. Sorption isotherms

Fig. 2 shows the effect of temperature in the scrutinized temperature range (25–45 °C) on the equilibrium moisture content. The sorptivity of the hydrogel beads was reduced when the temperature was increased. Even though differences in the moisture content are small between SA-NM (1:1) and SA-NM (1:1.5) hydrogels beads. In the case of SA-NM (1:0) beads, the difference in moisture content is more marked. These changes agree with the thermodynamics of sorption as adsorbed water is lowered with temperature (Adamiec, 2009). On the other hand, the equilibrium moisture content of the hydrogel beads increased at the same adsorption temperature as the amount of nopal mucilage increased. This behavior might be ascribed to the complex structure of biopolymers constituting the matrix of the hydrogel beads. The D-galacturonic acid and monosugars (e.g., D-xylose, D-galactose, L-rhamnose and L-arabinose) contained in nopal mucilage have great affinity and capacity to bind easily water molecules (Cortés-Camargo et al., 2017). Sodium alginate is composed mainly by glucuronic and mannuronic acids forming blocks alternating sequences also with high solubility and affinity by water (Benavides et al., 2016; Galus & Lenart, 2013).

Fig. 2a to 2. c shows a clear effect of the content of sesame oil in the different systems hydrogels beads on the sorptivity of the dried beads. The equilibrium curves of the hydrogel beads with the SA-NM mixtures are well above the curves of the hydrogels formulated only with sodium alginate at the same oil content. This means that hydrogels with sodium alginate are less sensitive to water vapor in the environment, therefore, they are more stable to water activity, manifesting in a lower capacity for adsorption of water molecules by the blocking effect of oil microdroplets, which prevent water vapor molecules from accessing the sodium alginate sorption surface. Whilst in the case of hydrogels formulated with SA-NM mixtures, the amount of nopal mucilage present in these systems and its high hygroscopicity favors the gels structures being more plasticizing (Medina-Torres et al., 2013), which prevents oil

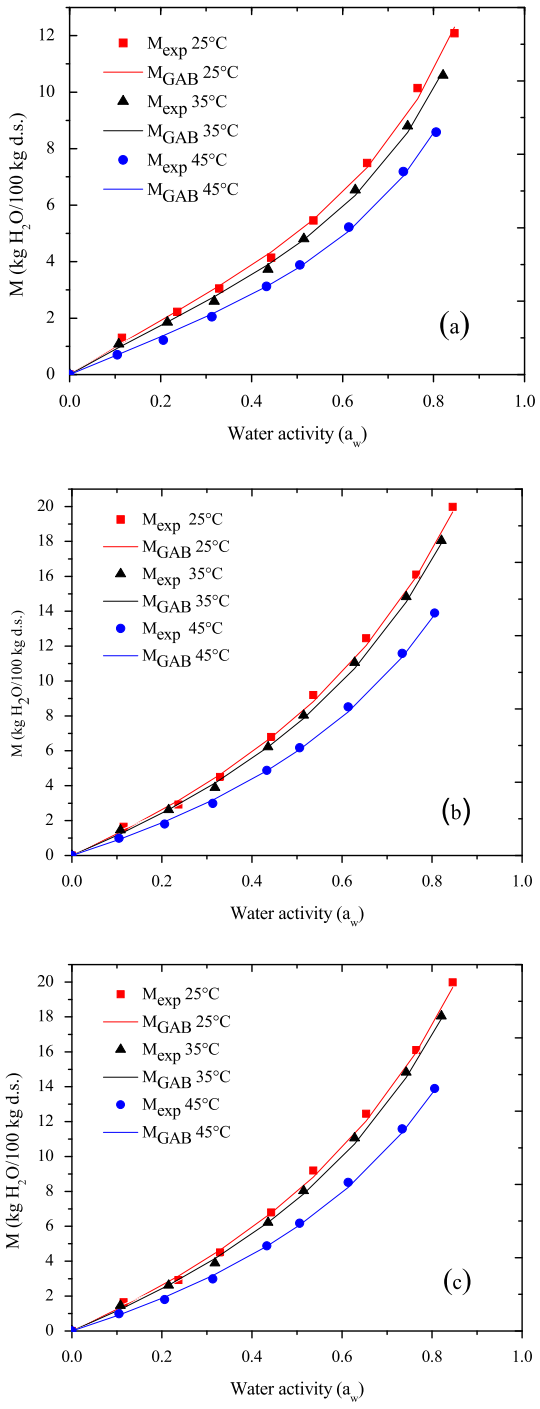

Fig. 2. Water sorption isotherms of sesame oil SA-NM hydrogel beads at 25, 35 and 45 °C for (a) SA-NM (1:0); (b) SA-NM (1:1) and (c) SA-NM (1:1.5).

molecules are capable of blocking or clogging the surface pores of hydrogels, promoting a higher moisture adsorption content.

A further important aspect to note is that the behavior of the sorption isotherms can be classified into three different regions independently of temperature. A first region where a monomolecular sorption occurs at low water activities values ($a_W < 0.4$). This region represents water molecules that are strongly bounded to the sorption material and having vaporization enthalpy that is higher than that of pure water. The sorption of water onto material surfaces containing highly hydrophilic biopolymers (e.g., proteins and polysaccharides) is a distinctive instance of such behavior. In such case, the moisture content reflects the adsorption of the first layer (Al-Muhtaseb et al., 2002). A second region is linked to

Table 1
Estimated GAB parameters for sesame oil SA – NM hydrogel beads.

System	Parameters	25 °C	35 °C	45 °C
SA-NM (1:0)	M_0	4.61 ± 0.21^{a}	4.13 ± 0.22^{ab}	3.61 ± 0.22^{b}
	C	2.80 ± 0.05^{a}	2.76 ± 0.08^{a}	2.29 ± 0.08^{b}
	K	0.80 ± 0.04^{a}	0.82 ± 0.04^{a}	0.82 ± 0.06^{a}
	R^2	0.998	0.998	0.999
	E (%)	3.92	3.66	3.20
SA-NM (1:1)	M_0	12.50 ± 0.57^{a}	11.49 ± 0.62^{ab}	10.09 ± 0.62^{b}
	C	1.37 ± 0.03^{a}	1.33 ± 0.04^{a}	1.17 ± 0.04^{b}
	K	0.69 ± 0.03^{a}	0.71 ± 0.04^{a}	0.70 ± 0.05^{a}
	R^2	0.999	0.999	0.999
	E (%)	4.24	3.76	3.59
SA-NM (1:1.5)	M_0	12.57 ± 0.57^{a}	11.64 ± 0.63^{ab}	10.42 ± 0.64^{b}
	C	1.55 ± 0.03^{a}	1.54 ± 0.05^{a}	1.32 ± 0.04^{b}
	K	0.70 ± 0.03^{a}	0.73 ± 0.04^{a}	0.72 ± 0.05^{a}
	R^2	0.999	0.999	0.999
	E (%)	3.92	3.91	3.22

*SA: sodium alginate; NM: nopal mucilage; M_0: moisture content of the monolayer (kg water/100 kg d.s; C and K: GAB model constants; a_W: Water activity; R^2: coefficient of linear determination; E: mean relative deviation modulus (%).
**Results are presented as means ± SD (n = 3).
***Values with different letters in the same row indicate significant difference ($p \leq 0.05$).

a semi-linear behavior displayed at $0.4 < a_W < 0.65$, which is distinctive of multilayer sorption. Here, sugars contained in nopal mucilage retain the largest fraction of water molecules, but the molecules conforming the SA-NM hydrogel beads contain sufficient water molecules to reduce the initial rigidity (Tsami et al., 1992). A third region where a sharp increase in equilibrium moisture content in the range of a_W of 0.65–0.85 was observed due to capillary condensation (Ciurzyńska et al., 2019; Tsami et al., 1992). Therefore, it can be said that the isotherms of these hydrogel beads fall within a behavior Type II isotherms (sigmoidal shape) (Al-Muhtaseb et al., 2002; Blahovec & Yanniotis, 2009; Brunauer et al., 1938).

Table 1 reports the estimated parameters M_0, C and K obtained by least-squares fitting the experimental sorption data of the GAB model. An accurate description of the experimental data was obtained with the GAB model, with mean relative modulus values (E) smaller than 5% and R^2 values non-smaller than 0.998 for all cases and types of hydrogel beads (Monte et al., 2018). The parameter M_0 is commonly considered as an optimal value at which a food product is more stable. This parameter reflects the fraction of water molecules that are strongly linked to specific sites (Hoyos-Leyva et al., 2018). Table 1 shows that the M_0 values have a negative trend with the temperature, which can be attributed to structural changes in biopolymers matrix. In fact, increased adsorption temperatures reduce decrease the number of active sites where water can be adsorbed. The level of the activation energy with increasing temperature, becoming relatively unstable and breaking down the bonds between adsorption sites and water molecules (Lago & Noreña, 2015). A similar pattern was observed for microcapsules containing rosemary essential oil (0.124–0.084 kg H_2O/100 kg d.s.), date syrup (0.186–0.065 kg H_2O/100 kg d.s.) as well as for unsaturated fatty acids concentrates nanocapsules (0.105–0.079 kg H_2O/100 kg d.s.) (Esquerdo et al., 2019; Farahnaky et al., 2016; Silva et al., 2014). The values of the monolayer (M_0) of hydrogels beads were significantly lower for SA-NM (1:0) beads (4.61–3.61 kg H_2O/100 kg d.s.) than for SA-NM (1:1 and 1:1.5) hydrogel beads (12.57–10.09 kg H_2O/100 kg d.s.) which indicates that nopal mucilage gave more number of sites available for water binding in the hydrogel beads. Furthermore, the variation between the monolayer values can be attributed to structural and topological changes in the sorption surface that the different types of hydrogel beads undergo when dehydrated by forced air convection during their elaboration.

The Guggenheim's parameter C reflects the binding strength of sorption molecules to primary active sites. The results in Table 1 showed

Table 2
Surface area of sorption (m^2/g) for sesame oil SA – NM hydrogel beads.

	25 °C	35 °C	45 °C
SA-NM (1:0)	161.26 ± 7.33^{a}	144.51 ± 7.82^{ab}	126.26 ± 7.72^{b}
SA-NM (1:1)	437.37 ± 19.90^{a}	402.22 ± 21.70^{ab}	353.13 ± 21.60^{b}
SA-NM (1:1.5)	440.09 ± 20.00^{a}	407.51 ± 22.00^{ab}	364.58 ± 22.30^{b}

*SA: sodium alginate; NM: nopal mucilage.
**Results are presented as means ± SD (n = 3).
***Values with different letters in the same row indicate significant difference ($p \leq 0.05$).

that the parameter *C* decreased with the sorption temperature, a behavior that can be explained by recalling that adsorbent-adsorbate interactions are exothermic (Diosady et al., 1996). The values of parameter *C* for SA-NM (1:0) beads were found in the range of 2.29–2.80; while for SA-NM (1:1 and 1:1.5) hydrogels beads were found between 1.17 and 1.55. These results suggest that parameter *C* can be linked to the heat of adsorption. In the case of sodium alginate beads, the bonds between the monolayer water and the available binding sites of the beads were the highest, which in turn suggests that the stability of adsorbed water molecules on the surface of the beads was enhanced (Hoyos-Leyva et al., 2018; Timmermann, 2003). It has been pointed out that the parameter *C* might lack lacks any physical interpretation, and it is only a fitting parameter playing the role of a compensatory effect for the different parameters in fitting (Alpizar-Reyes et al., 2017).

The Guggenheim's parameter *K* represents multilayer-adsorbent interactions, and its values are contained between the monolayer and liquid water energies (Pérez-Alonso et al., 2006). The theory underlying the GAB model indicates that the water monolayer is tightly bounded to the surface, whereas the multilayers are weakly attracted by the solid. Molecules that are not directly attached to the solid surface exhibit physical properties similar to that of pure water (Liébanes et al., 2006). In this study, all the values of the parameter *K* for the three types of SA-NM hydrogel beads were lower than one and ranged between 0.69 and 0.82, which implies a better-structured state of the water molecules in the layer adjacent to the monolayer of the beads. This effect involves water molecules that are highly ordered, such that the mobility is strongly constrained. As such, the availability of water molecules for deterioration and spoilage of hydrogel beads is constrained (Hoyos-Leyva et al., 2018).

3.3. Sorption properties of sesame oil hydrogel beads

The relative number and diameter of pores determines the total area of sorption and, the pore's surface properties influence the hydration rate (Velázquez-Gutiérrez et al., 2015). The estimated surface areas of sorption for the three types of hydrogel beads are shown in Table 2, showing a decrease in surface area of sorption when temperature increased due to the reduction in availability of active sites and also in binding energies to water sorption (Alpizar-Reyes et al., 2017). The hydrogel beads that contained nopal mucilage had values that ranged between 353 and 440 m^2/g, which were significantly higher than the results obtained for pure sodium alginate beads (126 and 161 m^2/g). These results indicate an increase the number of active sites that area available for hydrophilic binding when nopal mucilage was added, a behavior that can be attributed to the higher concentration of hydroxyl groups in nopal mucilage structure which gives a high affinity for water (León-Martínez et al., 2010). Commonly, food products have a surface area of sorption ranged between 100 and 250 m^2/g; higher values indicate that the hydrocolloids had an intrinsic microporous structure (Alpizar-Reyes et al., 2017).

The pore radius (r_p) values of hydrogel beads ranged from 0.81 to 7.59 nm (Table 3) for different water activities, temperatures and wall material ratios. This interval corresponds to micropores (<2 nm) and mesopores (2–50 nm) (Velázquez-Gutiérrez et al., 2015). In this study, one has micropores at water activities smaller than 0.5. The pore radius values of the hydrogel beads were similar for the same water activity value and temperature regardless of the type of wall material used. The effect was probably due to the use of the same method of drying in the conformation of the beads. During the drying process by forced air convection, the extraction of water from the beads produces an internal and external pressure gradient, which leads to changes in the internal structure of the hydrogel beads. Sundaram and Durance (2008) showed the formation of interconnected pores in the internal structure of gels with locust bean gum – pectin – starch dehydrated by air convection.

On the other hand, the transport mechanisms in the solid bulk are strongly dependent on the structural characteristics of the porous matrix, the dimensional properties of pores and the surface heterogeneity. In particular, the surface heterogeneity is expressed at low water activity under sub-monomolecular coverage, involving the presence of structural defects and/or chemical disorder (Zelenka, 2016). For microporous structures, the diffusional transport is limited by interactions between the pore walls and the sorption molecules (i.e., entropic and

Table 3
Pore radius (nm) for different water activities, temperatures and wall material SA – NM ratios of sesame oil hydrogel beads.

a_W	SA - NM (1:0)			SA - NM (1:1)			SA - NM (1:1.5)		
	25 °C	35 °C	45 °C	25 °C	35 °C	45 °C	25 °C	35 °C	45 °C
0.05	0.82 ± 0.10^{a}	0.82 ± 0.03^{a}	1.05 ± 0.14^{a}	0.82 ± 0.10^{a}	0.81 ± 0.21^{a}	1.08 ± 0.26^{a}	0.84 ± 0.08^{b}	0.82 ± 0.10^{b}	1.12 ± 0.07^{a}
0.10	0.93 ± 0.04^{a}	0.92 ± 0.24^{a}	1.11 ± 0.22^{a}	0.94 ± 0.24^{a}	0.92 ± 0.18^{a}	1.14 ± 0.13^{a}	0.95 ± 0.07^{a}	0.92 ± 0.18^{a}	1.17 ± 0.15^{a}
0.15	1.04 ± 0.12^{a}	1.02 ± 0.23^{a}	1.17 ± 0.23^{a}	1.04 ± 0.14^{a}	1.02 ± 0.18^{a}	1.20 ± 0.25^{a}	1.05 ± 0.07^{a}	1.02 ± 0.07^{a}	1.23 ± 0.16^{a}
0.20	1.16 ± 0.21^{a}	1.12 ± 0.05^{a}	1.25 ± 0.10^{a}	1.16 ± 0.14^{a}	1.12 ± 0.05^{a}	1.27 ± 0.03^{a}	1.16 ± 0.04^{a}	1.13 ± 0.23^{a}	1.30 ± 0.25^{a}
0.25	1.28 ± 0.05^{a}	1.24 ± 0.13^{a}	1.33 ± 0.06^{a}	1.28 ± 0.10^{a}	1.24 ± 0.19^{a}	1.35 ± 0.18^{a}	1.28 ± 0.26^{a}	1.24 ± 0.12^{a}	1.38 ± 0.06^{a}
0.30	1.41 ± 0.05^{a}	1.36 ± 0.25^{a}	1.42 ± 0.23^{a}	1.41 ± 0.17^{a}	1.36 ± 0.24^{a}	1.44 ± 0.03^{a}	1.41 ± 0.25^{a}	1.36 ± 0.05^{a}	1.47 ± 0.20^{a}
0.35	1.56 ± 0.23^{a}	1.50 ± 0.20^{a}	1.53 ± 0.16^{a}	1.56 ± 0.09^{a}	1.50 ± 0.10^{a}	1.55 ± 0.06^{a}	1.56 ± 0.26^{a}	1.50 ± 0.08^{a}	1.57 ± 0.07^{a}
0.40	1.73 ± 0.25^{a}	1.66 ± 0.03^{a}	1.66 ± 0.09^{a}	1.73 ± 0.04^{a}	1.67 ± 0.20^{a}	1.68 ± 0.06^{a}	1.73 ± 0.19^{a}	1.66 ± 0.06^{a}	1.69 ± 0.07^{a}
0.45	1.93 ± 0.17^{a}	1.85 ± 0.10^{a}	1.81 ± 0.09^{a}	1.93 ± 0.11^{a}	1.85 ± 0.17^{a}	1.82 ± 0.13^{a}	1.92 ± 0.24^{a}	1.85 ± 0.07^{a}	1.84 ± 0.16^{a}
0.50	2.17 ± 0.07^{a}	2.07 ± 0.15^{a}	1.99 ± 0.09^{a}	2.17 ± 0.18^{a}	2.07 ± 0.18^{a}	2.00 ± 0.03^{a}	2.15 ± 0.08^{a}	2.07 ± 0.23^{a}	2.02 ± 0.13^{a}
0.55	2.45 ± 0.24^{a}	2.33 ± 0.08^{a}	2.21 ± 0.10^{a}	2.45 ± 0.26^{a}	2.34 ± 0.16^{a}	2.22 ± 0.06^{a}	2.43 ± 0.19^{a}	2.33 ± 0.08^{a}	2.23 ± 0.20^{a}
0.60	2.79 ± 0.22^{a}	2.66 ± 0.05^{a}	2.48 ± 0.23^{a}	2.79 ± 0.20^{a}	2.67 ± 0.12^{a}	2.49 ± 0.25^{a}	2.77 ± 0.07^{a}	2.66 ± 0.13^{a}	2.50 ± 0.17^{a}
0.65	3.23 ± 0.24^{a}	3.08 ± 0.26^{a}	2.84 ± 0.05^{a}	3.23 ± 0.20^{a}	3.08 ± 0.14^{ab}	2.84 ± 0.04^{b}	3.21 ± 0.17^{a}	3.07 ± 0.22^{a}	2.85 ± 0.10^{a}
0.70	3.80 ± 0.20^{a}	3.62 ± 0.15^{ab}	3.31 ± 0.20^{b}	3.80 ± 0.12^{a}	3.63 ± 0.22^{a}	3.31 ± 0.25^{a}	3.78 ± 0.04^{a}	3.61 ± 0.18^{ab}	3.31 ± 0.21^{b}
0.75	4.58 ± 0.23^{a}	4.37 ± 0.10^{ab}	3.97 ± 0.07^{b}	4.58 ± 0.20^{a}	4.37 ± 0.20^{ab}	3.97 ± 0.07^{b}	4.57 ± 0.12^{a}	4.36 ± 0.11^{a}	3.96 ± 0.16^{b}
0.80	5.71 ± 0.21^{a}	5.46 ± 0.20^{a}	4.96 ± 0.07^{b}	5.72 ± 0.10^{a}	5.45 ± 0.07^{b}	4.95 ± 0.03^{c}	5.72 ± 0.03^{a}	5.46 ± 0.09^{a}	4.93 ± 0.17^{b}
0.85	7.51 ± 0.19^{a}	7.21 ± 0.12^{a}	6.61 ± 0.11^{b}	7.52 ± 0.18^{a}	7.18 ± 0.13^{a}	6.59 ± 0.21^{b}	7.59 ± 0.19^{a}	7.22 ± 0.08^{a}	6.55 ± 0.21^{b}

*SA: sodium alginate; NM: nopal mucilage.
**Results are presented as means ± SD (n = 3).
***Values with different letters in the same row indicate significant difference ($p \leq 0.05$).

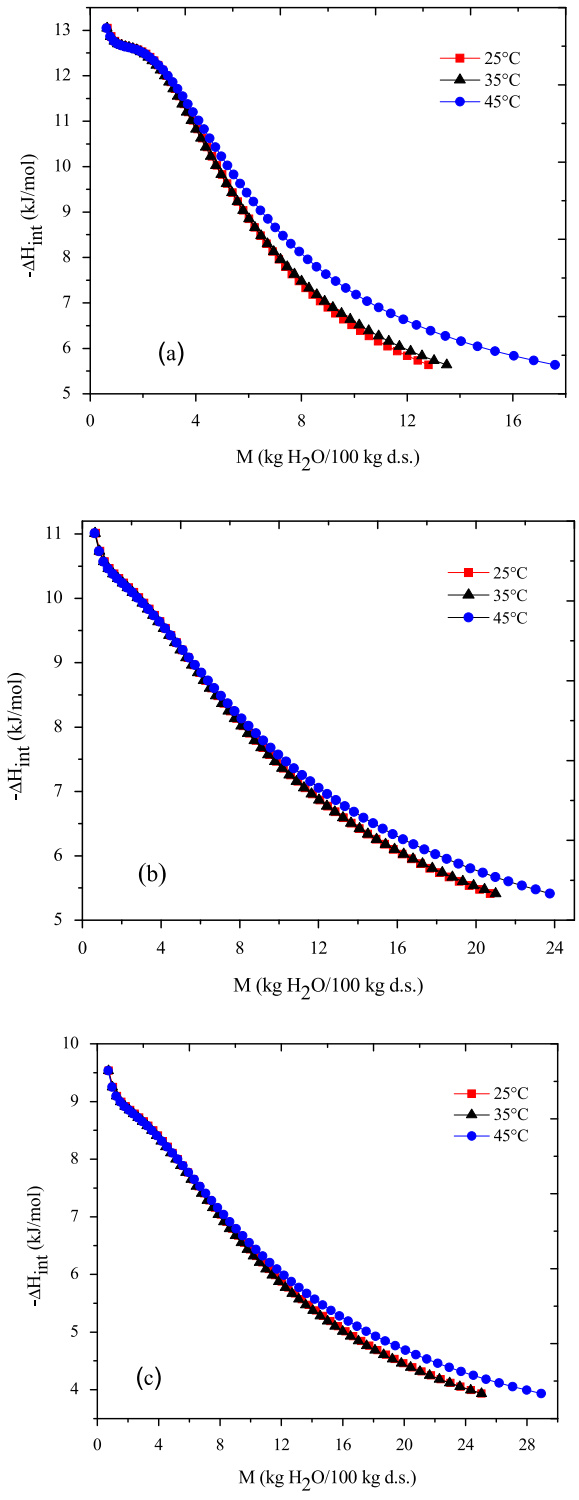

Fig. 3. Integral enthalpy as a function of moisture content of sesame oil SA-NM hydrogel beads at 25, 35 and 45 °C for (a) SA-NM (1:0); (b) SA-NM (1:1) and (c) SA-NM (1:1.5).

steric effects) as porous walls are barriers blocking the mobility. In contrast, surface and capillary forces become important in mesoporous structures (Alpizar-Reyes et al., 2017; Azuara & Beristain, 2006). Additionally, the local temperature patterns may affect the interchange of water molecules (Kapsalis, 1981).

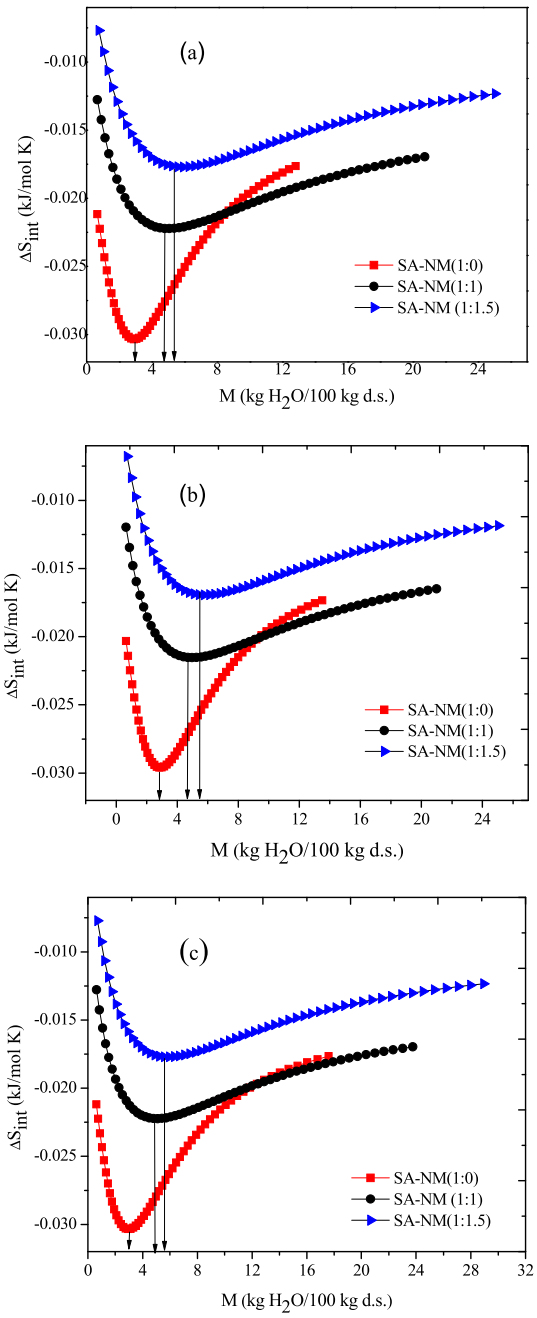

Fig. 4. Integral entropy as a function of moisture content of sesame oil SA-NM hydrogel beads at 25, 35 and 45 °C for (a) SA-NM (1:0); (b) SA-NM (1:1) and (c) SA-NM (1:1.5).

3.4. Effect of the wall materials on the thermodynamic properties of sesame oil hydrogel beads

Sorption properties described well the point where the monolayer moisture content (M_0) allows the maximum quantity of water molecules yielded primarily to the surface of beads. At such point, the beads adsorb the maximum level of water molecules. To achieve the understanding of the adsorption phenomenon in the whole system, a study of the thermodynamic properties is mandatory, where the second principle of thermodynamics allows us to ensure that the point of maximum stability will be found in the region where the entropy, determined by the integral method, has the minimum value. Maximum enthalpy reflects that the water molecule layers has maximum covering of strong binding sites and strong water-solid interactions. Hence, a decrease in enthalpy

Table 4
Maximum stability conditions of sesame oil SA – NM hydrogel beads.

SA – NM	1:0	1:1	1:1.5
25 °C			
M	3.31 ± 0.24^{c}	4.52 ± 0.50^{b}	4.71 ± 0.19^{a}
a_W	0.35 ± 0.24^{b}	0.45 ± 0.24^{a}	0.59 ± 0.24^{a}
35 °C			
M	3.42 ± 0.47^{c}	4.99 ± 0.69^{b}	5.44 ± 0.93^{a}
a_W	0.25 ± 0.05^{c}	0.38 ± 0.07^{b}	0.47 ± 0.02^{a}
45 °C			
M	3.64 ± 0.18^{b}	5.09 ± 0.48^{b}	5.59 ± 1.05^{a}
a_W	0.23 ± 0.03^{c}	0.36 ± 0.09^{b}	0.48 ± 0.04^{a}

*SA: sodium alginate; NM: nopal mucilage; M: moisture content (kg H_2O/100 kg d.s.); a_W: Water activity.
**Results are presented as means ± SD (n = 3).
***Values with different letters in the same row indicate significant difference ($p \leq 0.05$).

reflects less active adsorption sites covered and the formation of multilayers (Alpizar-Reyes et al., 2017). The variation of integral enthalpy $(\Delta H)_{int}$ is shown in Fig. 3. The enthalpy decreased the moisture content increased in the beads, which is an indication that available sites for water sorption are less active, hence resulting in a weaker energetic interactions by water molecules – water molecules and surface – water molecules (Hoyos-Leyva et al., 2018; Vasile et al., 2020). On this context, one can postulate that SA - NM hydrogel beads had lower energetic interactions with a softer curve, indicating higher stability than sodium alginate beads (Viganó et al., 2012). The effect of the nopal mucilage upon a higher thermal stability of beads is beneficiated by the presence of proteins from nopal mucilage, which incorporate an amphiphilic character to the wall matrix (Ravi et al., 2019).

Enthalpy gives some interesting information on energetic variations at given hydration values (Viganó et al., 2012). In contrast, entropy is an index of disordered patterns of water molecules adsorbed on the hydrogel. In this way, the minimum zone of entropy reflects the maximum stability conditions since strongest bonds between hydrogel – water molecules appear at such conditions. Indeed, ordered water molecules becomes less available to participate in deterioration reactions (Hoyos-Leyva et al., 2018; Al-Muhtaseb et al., 2002). Fig. 4 presents the variation of the integral entropy with respect to the moisture content at 25, 35 and 45 °C. The hydrogel beads exhibit a decrement of the integral entropy, achieve a minimum to subsequently increase as moisture content increased. Decreased values of the integral entropy are linked to increased restrictions of water molecules mobility since available sites are saturated and even higher energy sites are increasingly occupied. A subsequent increase indicates the availability of water molecules to adsorb as multilayers. Entropy will display values like that of liquid water for higher moisture contents (Hoyos-Leyva et al., 2018; Lara et al., 2020). Negative values of ΔS_{int} can be related to the presence of a diversity of polar groups with the ability of binding with water, which in turn is a reflect of strong hydrophilicity (Lara et al., 2020). The values of integral enthalpy were between −0.05 and −0.30 kJ/mol K, this value remains a little bit lower for oils that were microencapsulated in biopolymeric matrices, including gums, proteins and maltodextrins. In these cases, the microcapsules showed a diversity of integral entropy change (from 0.040 to −0.040 kJ/mol K) (Bonilla et al., 2010; Cano-Higuita et al., 2015; Koua et al., 2014).

The temperature effect over the hydrogel beads blends (see Fig. 4) has a close relationship with the behavior observed in the parameters of the GAB model. In fact, the integral enthalpy values increased for all hydrogel beads with the temperature increasing. The mobility of water molecules due to an increase of kinetic energy in the system promoted by higher temperatures is reflected in by such behavior (Alpizar-Reyes et al., 2017). The effect of the wall materials in the integral entropy of sesame oil hydrogel beads shows significant difference between SA-NM (1:0) beads and the beads SA-NM (1:1 and 1:1.5), an effect that might be

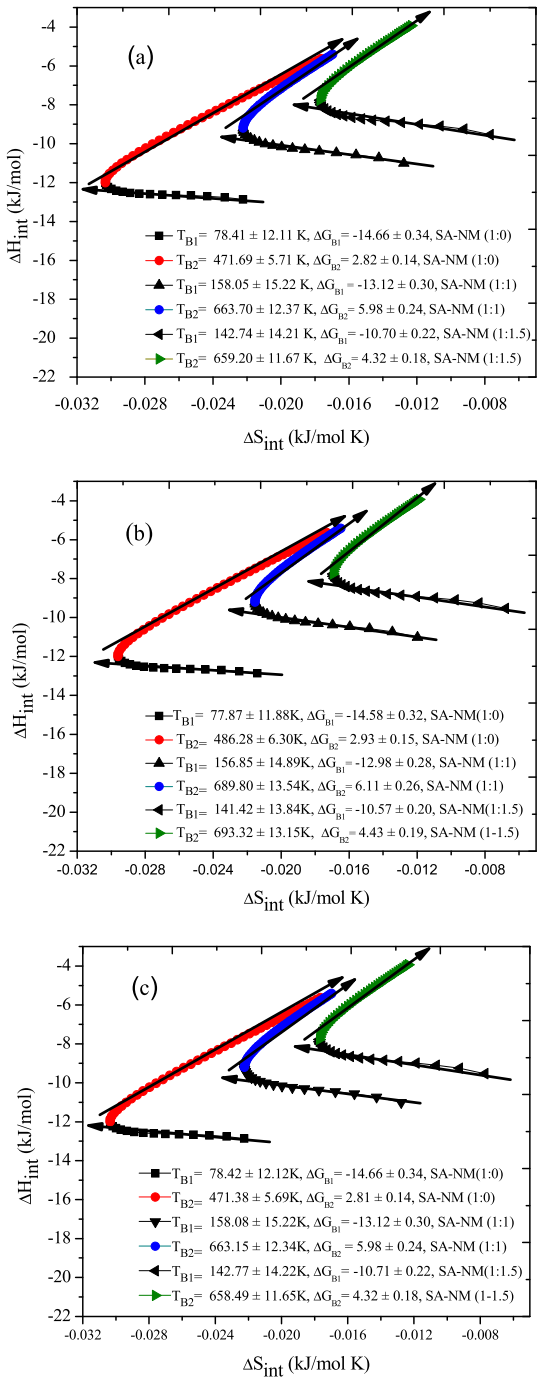

Fig. 5. Integral enthalpy–integral entropy compensation for water sorption in sesame oil SA-NM hydrogel beads at (a) 25 °C; (b) 35 °C and (c) 45 °C.

related to the core material and wall material chemistry conformation. Ravi et al. (2019) showed that nopal mucilage presents an amphiphilic character that allows the oil to bind with the mucilage, causing a more organized and structured system and less values on integral entropy. Therefore, the addition of nopal mucilage to the bead matrix improved the stability of sesame oil, leading to beads with higher stability and highest degree of protection against deteriorative factors of sesame oil.

The maximum stability shown in Table 4 was determined as the mean of lowest integral entropy values, with the corresponding moisture content and water activities. In fact, the lowest integral entropy values denote the condition at which the water molecules contain high order, such that these molecules are not available to induce spoilage reactions

(Ribeiro et al., 2016). The high moisture contents and water activities related with the maximum stability were achieved for SA-NM 1:1.5 beads, thus there is a clear beneficial effect on the addition of nopal mucilage to sodium alginate hydrogel beads as related with the matrix structure. The maximum stability moisture content for all beads showed a linear relation with respect to the temperature. This feature can be attained to the increment of temperature as a higher relaxed cross-linked matrix is promoted, which turn results into less interactions between sesame oil, biopolymers on the matrix and water molecules (Hoyos-Leyva et al., 2018). These results are in concordance with the monolayer moisture content values observed for different temperatures, as the amount of nopal mucilage increases in the composition of the wall material. Moreover, maximum stability moisture contents are located into the second region observed for the sorption isotherms, which is characteristic of a multilayer sorption (Tsami et al., 1992). Consequently, the effect of the wall materials on sesame oil hydrogel beads suggests that the sorption properties are directly related with the thermodynamic properties, and this relation between both phenomena can be studied with the isokinetic compensation theory.

3.5. Compensation theory

The enthalpy-entropy compensation theory, also called as isokinetic compensation theory, is commonly used to assess water sorption mechanisms and sorption reactions (Azuara & Beristain, 2006). The theory provides a framework to evaluate interactions of water molecules with food components, leading to increased order (related to enthalpy) over disorganization, and increased freedom of water molecules (related to entropy) (Spada et al., 2013). The approach is applied only when the isokinetic temperature (T_B) differs from the harmonic mean temperature (T_{hm}) (Krug et al., 1976a,b). Fig. 5 presents the enthalpy-entropy compensation results obtained by showing the integral properties at 25, 35 and 45 °C. All hydrogel bead formulations presented two lines. The first line at low moisture contents (0–2.89 kg H_2O/100 kg d.s.) with $T_{B1} = 78.41 \pm 12.11$ K $T_{B1} = 77.87 \pm 11.88$ K and $T_{B1} = 78.42 \pm 12.12$ K for the system SA-NM (1:0) at 25, 35 and 45 °C, respectively. In the range of moisture content (0–5.10 kg H_2O/100 kg d.s.) and temperature (25–45 °C) of the SA-NM system (1:1), the values of T_{B1} were between 156.85 ± 14.89 K and 158.08 ± 15.22 K. For the SA-NM system (1:1.5) in the range of moisture content (0–5.95 kg H_2O/100 kg d.s.), the T_{B1} values were found between 141.42 ± 13.84 K and 142.77 ± 14.22 K in the range temperature studied. The second line is specific to each hydrogel beads system. For the SA-NM system (1:0), the T_{B2} values were found between 471.69 ± 5.71 K and 486.28 ± 6.30 K in the range temperature studied. The T_{B2} values of the SA-NM system (1:1) were 663.70 ± 12.37 K, 689.80 ± 13.54 K and 663.15 ± 12.34 K at 25, 35 and 45 °C, respectively. Finally, for the SA-NM system (1:1.5), the T_{B2} values were found between 658.49 ± 11.65 K and 693.32 ± 13.15 K in the range temperature studied.

The fulfilment of the isokinetic theory was verified since the mean harmonic temperature (T_{hm}) was 307.93 K, which was different from the T_B's. Following Leffler (1955), it is suggested that entropy-driven mechanisms control the sorption process ($T_B < T_{hm}$) for low moisture content. At minimum entropy conditions, an entropy-enthalpy equilibrium is present. However, the sorption process is dominated by enthalpy-driven mechanisms ($T_B > T_{hm}$) after minimum integral entropy. Other reports found similar behaviors for different foods, for which the adsorption process was dominated by entropic mechanisms for water molecules adsorbed (Azuara & Beristain, 2006; Silva et al., 2014).

The free energy change (ΔG_B) provides information on the water molecules – hydrogel beads affinity by showing whether the moisture sorption is a spontaneous (-ΔG_B) or non-spontaneous (+ΔG_B) mechanism (Apostolopoulos & Gilbert, 1990). In our case, the ΔG_{B1} values were between −14.66 ± 0.34 kJ/mol and −10.57 ± 0.20 kJ/mol for three systems of hydrogel beads at 25, 35 and 45 °C. These results demonstrate that the adsorption process at low moisture contents is spontaneous, showing the affinity between the molecules of the water vapor and the hydrogel beads in the studied temperature range. In contrast, the ΔG_{B2} values were between 2.81 ± 0.14 kJ/mol and 6.11 ± 0.26 kJ/mol for moisture contents higher than 5.92 kg H_2O/100 kg d.s. These values of (+ΔG_B) imply that adsorption is not spontaneous, which in turn suggests that the hydrogel beads is unable to absorb moisture from the environment, an effect that is desirable to have stable beads (Cladera-Olivera, 2011; Hidar et al., 2018).

4. Conclusions

The adsorption isotherms of the hydrogel beads presented a sigmoidal shape that is commonly found in food materials. The equilibrium moisture contents showed a marked reduction with increase in temperature over the whole range of water activity. The well-known GAB equation showed good accuracy to modelling moisture sorption of the hydrogel beads in a water activity range of 0.11–0.85 and temperatures of 25, 35 and 45 °C. On the other hand, the pore radius of the hydrogel beads presented values in the range from 0.81 to 7.59 nm, which can be classified as mesopores and micropores. On the other hand, the minimum integral entropy was considered as an index for addressing the suitable conditions for storage. It was found that the suitable values of water activity were in the range of 0.23–0.59 for the scrutinized temperatures. Finally, the enthalpy-entropy compensation theory indicated that the adsorption processes are driven by entropic processes for relatively low moisture contents values. In contrast, the sorption process is driven by enthalpy mechanisms for relatively high moisture content values. The information obtained from the analysis of sorption isotherms provided useful insights to develop stable nutraceutical systems encapsulated by ionic gelation.

CRediT authorship contribution statement

S.K. Velázquez-Gutiérrez: Conceptualization, Methodology, Software, Validation, Investigation, Data curation, Writing - original draft, Writing - review & editing, Supervision, Project administration. **E. Alpizar-Reyes:** Conceptualization, Methodology, Investigation, Resources, Formal analysis, Writing - original draft, Visualization, Project administration, Funding acquisition. **A.Y. Guadarrama-Lezama:** Conceptualization, Resources, Writing - original draft, Project administration, Funding acquisition. **J.G. Báez-González:** Conceptualization, Writing - original draft, Writing - review & editing, Visualization, Supervision. **J. Alvarez-Ramírez:** Validation, Formal analysis, Writing - original draft, Writing - review & editing, Resources. **C. Pérez-Alonso:** Conceptualization, Resources, Data curation, Writing - original draft, Writing - review & editing, Visualization, Supervision, Project administration, Funding acquisition.

Declaration of competing interest

The authors declare that they have no known competing financial interests or personal relationships that could have appeared to influence the work reported in this paper.

Acknowledgements

Partial financial support is acknowledged to the Universidad Autónoma del Estado de México (Grant 4738/2019/CIB). S.K. Velázquez-Gutiérrez received a scholarship (Number 481491) from CONACyT-Mexico.

References

Adamiec, J. (2009). Moisture sorption characteristics of peppermint oil microencapsulated by spray drying. *Drying Technology, 27*(12), 1363–1369. https://doi.org/10.1080/07373930903383695

Al-Muhtaseb, A. H., McMinn, W. A. M., & Magee, T. R. A. (2002). Moisture sorption isotherm characteristics of food products: A review. *Food and Bioproducts Processing: Transactions of the Institution of Chemical Engineers, Part C, 80*(2), 118–128. https://doi.org/10.1205/09603080252938753

Alpizar-Reyes, E., Carrillo-Navas, H., Romero-Romero, R., Varela-Guerrero, V., Alvarez-Ramírez, J., & Pérez-Alonso, C. (2017). Thermodynamic sorption properties and glass transition temperature of tamarind seed mucilage (Tamarindus indica L.). *Food and Bioproducts Processing, 101*, 166–176. https://doi.org/10.1016/j.fbp.2016.11.006

Alpizar-Reyes, Erik, Varela-Guerrero, V., Cruz-Olivares, J., Carrillo-Navas, H., Alvarez-Ramirez, J., & Pérez-Alonso, C. (2020). Microencapsulation of sesame seed oil by tamarind seed mucilage. *International Journal of Biological Macromolecules, 145*, 207–215. https://doi.org/10.1016/j.ijbiomac.2019.12.162

Apostolopoulos, D., & Gilbert, S. G. (1990). Water sorption of coffee solubles by frontal inverse gas chromatography: Thermodynamic considerations. *Journal of Food Science, 55*(2), 475–487. https://doi.org/10.1111/j.1365-2621.1990.tb06790.x

Azuara, E., & Beristain, C. I. (2006). Enthalpic and entropic mechanisms related to water sorption of yogurt. *Drying Technology, 24*, 1501–1507. https://doi.org/10.1080/07373930600961173

Bannikova, A., Evteev, A., Pankin, K., Evdokimov, I., & Kasapis, S. (2018). Microencapsulation of fish oil with alginate: In-vitro evaluation and controlled release. *Lebensmittel-Wissenschaft & Technologie, 90*(December 2017), 310–315. https://doi.org/10.1016/j.lwt.2017.12.045

Benavides, S., Cortés, P., Parada, J., & Franco, W. (2016). Development of alginate microspheres containing thyme essential oil using ionic gelation. *Food Chemistry, 204*, 77–83. https://doi.org/10.1016/j.foodchem.2016.02.104

Beristain, C. I., Garcia, H. S., & Azuara, E. (1996). Enthalpy–entropy compensation in food vapor adsorption. *Journal of Food Engineering, 30*, 405–415. https://doi.org/10.1016/S0260-8774(96)00011-8

Blahovec, J., & Yanniotis, S. (2009). Modified classification of sorption isotherms. *Journal of Food Engineering, 91*(1), 72–77. https://doi.org/10.1016/j.jfoodeng.2008.08.007

Bonilla, E., Azuara, E., Beristain, C. I., & Vernon-Carter, E. J. (2010). Food Hydrocolloids Predicting suitable storage conditions for spray-dried microcapsules formed with different biopolymer matrices. *Food Hydrocolloids, 24*(6–7), 633–640. https://doi.org/10.1016/j.foodhyd.2010.02.010

Brigante, F. I., Lucini Mas, A., Pigni, N. B., Wunderlin, D. A., & Baroni, M. V. (2020). Targeted metabolomics to assess the authenticity of bakery products containing chia, sesame and flax seeds. *Food Chemistry, 312*(December 2019), 126059. https://doi.org/10.1016/j.foodchem.2019.126059

Brunauer, S., Emmet, P. H., & Teller, E. (1938). Adsorption of gases in multimolecular layers. *Journal of the American Chemical Society, 60*(2), 309–319. https://doi.org/10.1021/ja01269a023

Cano-Higuita, D. M., Villa-Vélez, H. A., Telis-Romero, J., Váquiro, H. A., & Telis, V. R. N. (2015). Influence of alternative drying aids on water sorption of spray dried mango mix powders: A thermodynamic approach. *Food and Bioproducts Processing, 93*(June), 19–28. https://doi.org/10.1016/j.fbp.2013.10.005

Cassini, A. S., Marczak, L. D. F., & Noreña, C. P. Z. (2006). Water adsorption isotherms of texturized soy protein. *Journal of Food Engineering, 77*(1), 194–199. https://doi.org/10.1016/j.jfoodeng.2005.05.059

Ciurzyńska, A., Jasiorowska, A., Ostrowska-Ligęza, E., & Lenart, A. (2019). The influence of the structure on the sorption properties and phase transition temperatures of freeze-dried gels. *Journal of Food Engineering, 252*(February), 18–27. https://doi.org/10.1016/j.jfoodeng.2019.02.008

Cladera-Olivera, F., Marczak, L. D. F., Noreña, C. P. Z., & Pettermann, A. C. (2011). Modeling water adsorption isotherms of pinhão (*Araucaria angustifolia* seeds) flour and thermodynamic analysis of the adsorption process. *Journal of. Food Process Engineering, 34*, 826–843. https://doi.org/10.1111/j.1745-4530.2009.00437.x

Corso, M. P., Fagundes-Klen, M. R., Silva, E. A., Cardozo Filho, L., Santos, J. N., Freitas, L. S., & Dariva, C. (2010). Extraction of sesame seed (Sesamun indicum L.) oil using compressed propane and supercritical carbon dioxide. *The Journal of Supercritical Fluids, 52*(1), 56–61. https://doi.org/10.1016/j.supflu.2009.11.012

Cortés-Camargo, S., Cruz-Olivares, J., Barragán-Huerta, B. E., Dublán-García, O., Román-Guerrero, A., & Pérez-Alonso, C. (2017). Microencapsulation by spray drying of lemon essential oil: Evaluation of mixtures of mesquite gum–nopal mucilage as new wall materials. *Journal of Microencapsulation, 34*(4), 395–407. https://doi.org/10.1080/02652048.2017.1338772

Cortés-Camargo, S., Gallardo-Rivera, R., Barragán-Huerta, B. E., Dublán-García, O., Román-Guerrero, A., & Pérez-Alonso, C. (2018). Exploring the potential of mesquite gum–nopal mucilage mixtures: Physicochemical and functional properties. *Journal of Food Science, 83*(1), 113–121. https://doi.org/10.1111/1750-3841.13937

Diosady, L. L., Rizvi, S. S. H., Cai, W., & Jagdeo, D. J. (1996). Moisture sorption isotherms of canola meals, and applications to packaging. *Journal of Food Science, 61*(1), 204–208. https://doi.org/10.1111/j.1365-2621.1996.tb14760.x

Escalona-García, L. A., Pedroza-Islas, R., Natividad, R., Rodríguez-Huezo, M. E., Carrillo-Navas, H., & Pérez-Alonso, C. (2016). Oxidation kinetics and thermodynamic analysis of chia oil microencapsulated in a whey protein concentrate-polysaccharide matrix. *Journal of Food Engineering, 175*, 93–103. https://doi.org/10.1016/j.jfoodeng.2015.12.009

Esquerdo, V. M., Monte, M. L., & Pinto, L. A. de A. (2019). Microstructures containing nanocapsules of unsaturated fatty acids with biopolymers: Characterization and thermodynamic properties. *Journal of Food Engineering, 248*(December 2018), 28–35. https://doi.org/10.1016/j.jfoodeng.2018.12.015

Fan, K., Zhang, M., & Bhandari, B. (2019). Osmotic-ultrasound dehydration pretreatment improves moisture adsorption isotherms and water state of microwave-assisted vacuum fried purple-fleshed sweet potato slices. *Food and Bioproducts Processing, 115*, 154–164. https://doi.org/10.1016/j.fbp.2019.03.011

Farahnaky, A., Mansoori, N., Majzoobi, M., & Badii, F. (2016). Physicochemical and sorption isotherm properties of date syrup powder: Antiplasticizing effect of maltodextrin. *Food and Bioproducts Processing, 98*, 133–141. https://doi.org/10.1016/j.fbp.2016.01.003

Galus, S., & Lenart, A. (2013). Development and characterization of composite edible films based on sodium alginate and pectin. *Journal of Food Engineering, 115*(4), 459–465. https://doi.org/10.1016/j.jfoodeng.2012.03.006

Hidar, N., Ouhammou, M., Idlimam, A., Jaouad, A., Bouchdoug, M., Lamharrar, A., Kouhila, M., & Mahrouz, M. (2018). Investigation of water adsorption and thermodynamic properties of stevia powder. *Journal of Food Measurement and Characterization, 12*(4), 2615–2625. https://doi.org/10.1007/s11694-018-9879-0

Hoyos-Leyva, J. D., Bello-Perez, L. A., Agama-Acevedo, J. E., Alvarez-Ramirez, J., & Jaramillo-Echeverry, L. M. (2019). Characterization of spray drying microencapsulation of almond oil into taro starch spherical aggregates. *LWT - Food Science & Technology, 101*(54), 526–533. https://doi.org/10.1016/j.lwt.2018.11.079

Hoyos-Leyva, J. D., Bello-Pérez, L. A., & Alvarez-Ramirez, J. (2018). Thermodynamic criteria analysis for the use of taro starch spherical aggregates as microencapsulant matrix. *Food Chemistry, 259*(March), 175–180. https://doi.org/10.1016/j.foodchem.2018.03.130

Kapsalis, J. G. (1981). Moisture sorption hysteresis. In *Water activity: Influences on food quality* (pp. 143–177). Elsevier.

Koua, B. K., Koffi, P. M. E., Gbaha, P., & Toure, S. (2014). Thermodynamic analysis of sorption isotherms of cassava (Manihot esculenta). *Journal of Food Science & Technology, 51*(9), 1711–1723. https://doi.org/10.1007/s13197-012-0687-y

Krug, R. R., Hunter, W. G., & Grieger, R. A. (1976a). Enthalpy-entropy compensation. 1. Some fundamental statistical problems associated with the analysis of van't Hoff and Arrhenius data. *Journal of Physical Chemistry, 80*(21), 2335–2341. https://doi.org/10.1021/j100562a006

Krug, R. R., Hunter, W. G., & Grieger, R. A. (1976b). Enthalpy–entropy compensation 2. Separation of the chemical from the statistical effect. *Journal of Physical Chemistry, 80*(21), 2342–2351. http://doi.org/10.1021/j100562a007.

Labuza, T. P., Kaanane, A., & Chen, J. Y. (1985). Effect of temperature on the moisture sorption isotherms and water activity shift of two dehydrated foods. *Journal of Food Science, 50*(2), 385–392. https://doi.org/10.1111/j.1365-2621.1985.tb13409.x

Lago, C. C., & Noreña, C. P. Z. (2015). Thermodynamic analysis of sorption isotherms of dehydrated yacon (*Smallanthus sonchifolius*) bagasse. *Food Bioscience, 12*, 26–33. https://doi.org/10.1016/j.fbio.2015.07.001

Lara, B. R. B., Dias, M. V., Guimarães Junior, M., de Andrade, P. S., de Souza Nascimento, B., Ferreira, L. F., & Yoshida, M. I. (2020). Water sorption thermodynamic behavior of whey protein isolate/polyvinyl alcohol blends for food packaging. *Food Hydrocolloids, 103*(September 2019). https://doi.org/10.1016/j.foodhyd.2020.105710

Leffler, J. E. (1955). The enthalpy-entropy relationship and its implications for organic chemistry. *Journal of Organic Chemistry, 20*(9), 1202–1231. https://doi.org/10.1021/jo01126a009

León-Martínez, F. M., Méndez-Lagunas, L. L., & Rodríguez-Ramírez, J. (2010). Spray drying of nopal mucilage (*Opuntia ficus*-indica): Effects on powder properties and characterization. *Carbohydrate Polymers, 81*(4), 864–870. https://doi.org/10.1016/j.carbpol.2010.03.061

Liébanes, M. D., Aragón, J. M., Palancar, M. C., Arévalo, G., & Jiménez, D. (2006). Equilibrium moisture isotherms of two-phase solid olive oil by-products: Adsorption process thermodynamics. *Colloids and Surfaces A: Physicochemical and Engineering Aspects, 282–283*, 298–306. https://doi.org/10.1016/j.colsurfa.2006.03.025

Medina-Torres, L., Brito-De La Fuente, E., Torrestiana-Sanchez, B., & Katthain, R. (2000). Rheological properties of the mucilage gum (*Opuntia ficus* indica). *Food Hydrocolloids, 14*, 417–424. https://doi.org/10.1016/S0268-005X(00)00015-1

Medina-Torres, L., GarcÍa-Cruz, E. E., Calderas, F., González Laredo, R. F., Sánchez-Olivares, G., Gallegos-Infante, J. A., Rocha-Guzmán, N. E., & RodrÍguez-RamÍrez, J. (2013). Microencapsulation by spray drying of gallic acid with nopal mucilage (Opuntia ficus indica). *Lebensmittel-Wissenschaft und -Technologie- Food Science and Technology, 50*(2), 642–650. https://doi.org/10.1016/j.lwt.2012.07.038

Menin, A., Zanoni, F., Vakarelova, M., Chignola, R., Donà, G., Rizzi, C., Mainente, F., & Zoccatelli, G. (2018). Effects of microencapsulation by ionic gelation on the oxidative stability of flaxseed oil. *Food Chemistry, 269*, 293–299. https://doi.org/10.1016/j.foodchem.2018.06.144

Monte, M. L., Moreno, M. L., Senna, J., Arrieche, L. S., & Pinto, L. A. A. (2018). Moisture sorption isotherms of chitosan-glycerol films: Thermodynamic properties and microstructure. *Food Bioscience, 22*(February), 170–177. https://doi.org/10.1016/j.fbio.2018.02.004

Moraes, K., & Pinto, L. A. A. (2012). Desorption isotherms and thermodynamics properties of anchovy in natura and enzymatic modified paste. *Journal of Food Engineering, 110*(4), 507–513. https://doi.org/10.1016/j.jfoodeng.2012.01.012

Mudgil, D., & Barak, S. (2013). Composition, properties and health benefits of indigestible carbohydrate polymers as dietary fiber: A review. *International Journal of Biological Macromolecules, 61*, 1–6. https://doi.org/10.1016/j.ijbiomac.2013.06.044

Nunes, R. V., & Rotstein, E. (1991). Thermodynamics of the water-foodstuff equilibrium. *Drying Technology, 9*(1), 113–137. https://doi.org/10.1080/07373939108916643

Paddon-Jones, D., Campbell, W. W., Jacques, P. F., Kritchevsky, S. B., Moore, L. L., Rodriguez, N. R., & Van Loon, L. J. C. (2015). Protein and healthy aging. *American*

Journal of Clinical Nutrition, 101(6), 1339S–1345S. https://doi.org/10.3945/ajcn.114.084061

Pérez-Alonso, C., Beristain, C. I., Lobato-Calleros, C., Rodríguez-Huezo, M. E., & Vernon-Carter, E. J. (2006). Thermodynamic analysis of the sorption isotherms of pure and blended carbohydrate polymers. *Journal of Food Engineering, 77*(4), 753–760. https://doi.org/10.1016/j.jfoodeng.2005.08.002

Ravi, A., Vijayanand, S., Rajeshkannan, V., Aisverya, S., Sangeetha, K., Sudha, P. N., & Hemapriya, J. (2019). *Alginates in comestibles. Alginates: Applications in the Biomedical and food industries* (Vol. 263).

Ribeiro, A. J., De Souza, F. R. L., Bezerra, J. M. N. A., Oliveira, C., Nadvorny, D., De La Roca Soares, M. F., Nunes, L. C. C., Silva-Filho, E. C., Veiga, F., & Soares Sobrinho, J. L. (2016). Gums' based delivery systems: Review on cashew gum and its derivatives. *Carbohydrate Polymers, 147*, 188–200. https://doi.org/10.1016/j.carbpol.2016.02.042

Rivera-Corona, J. L., Rodríguez-González, F., Rendón-Villalobos, R., García-Hernández, E., & Solorza-Feria, J. (2014). Thermal, structural and rheological properties of sorghum starch with cactus mucilage addition. *Lebensmittel-Wissenschaft und -Technologie- Food Science and Technology, 59*(2P1), 806–812. https://doi.org/10.1016/j.lwt.2014.06.011

Rodea-González, D. A., Cruz-Olivares, J., Román-Guerrero, A., Rodríguez-Huezo, M. E., Vernon-Carter, E. J., & Pérez-Alonso, C. (2012). Spray-dried encapsulation of chia essential oil (Salvia hispanica L.) in whey protein concentrate-polysaccharide matrices. *Journal of Food Engineering, 111*(1), 102–109. https://doi.org/10.1016/j.jfoodeng.2012.01.020

Rodríguez-Bernal, J. M., Flores-Andrade, E., Lizarazo-Morales, C., Bonilla, E., Pascual-Pineda, L. A., Gutierréz-López, G., & Quintanilla-Carvajal, M. X. (2015). Moisture adsorption isotherms of the borojó fruit (Borojoa patinoi. Cuatrecasas) and gum Arabic powders. *Food and Bioproducts Processing, 94*, 187–198. https://doi.org/10.1016/j.fbp.2015.03.004

Rosa, G. S., Moraes, M. A., & Pinto, L. A. A. (2010). Moisture sorption properties of chitosan. *Lebensmittel-Wissenschaft und -Technologie- Food Science and Technology, 43*(3), 415–420. https://doi.org/10.1016/j.lwt.2009.09.003

Sáenz, C., Sepúlveda, E., & Matsuhiro, B. (2004). Opuntia spp. mucilage's: A functional component with industrial perspectives. *Journal of Arid Environments, 57*, 275–290. https://doi.org/10.1016/S0140-1963(03)00106-X

Santiago-Lorenzo, M. R., López-Jiménez, A., Saucedo-Veloz, C., Cortés-Flores, J. I., Jaén-Contreras, D., & Suárez-Espinosa, J. (2016). Nutritional composition of tender cactus stems produced under mineral and organic fertilization. *Revista Fitotecnia Mexicana, 39*(4), 403–407. https://doi.org/10.35196/rfm.2016.4.403-407

Schneider, A. S. (1981). Hydration of biological membranes. In L. B. Rockland, & G. F. Stewart (Eds.), *Water activity influences on food quality* (pp. 338–405). New York: Academic Press.

Sepúlveda, E., Sáenz, C., Aliaga, E., & Aceituno, C. (2007). Extraction and characterization of mucilage in Opuntia spp. *Journal of Arid Environments, 68*(4), 534–545. https://doi.org/10.1016/j.jaridenv.2006.08.001

Shahidi, F., & Zhong, Y. (2005). Lipid oxidation: Measurement methods. In *Bailey's industrial oil and fat products*. Wiley. https://doi.org/10.1002/047167849x.bio050.

Silva, E. K., Fernandes, R., Borges, S. V., Botrel, D. A., & Queiroz, F. (2014). Water adsorption in rosemary essential oil microparticles: Kinetics, thermodynamics and storage conditions. *Journal of Food Engineering, 140*, 39–45. https://doi.org/10.1016/j.jfoodeng.2014.05.003

Singh, R. R. B., Rao, K. H., Anjaneyulu, A. S. R., & Patil, G. R. (2006). Water desorption characteristics of raw goat meat: Effect of temperature. *Journal of Food Engineering, 75*, 228–236. https://doi.org/10.1016/j.jfoodeng.2005.04.013

Sonwane, C. G., & Bhatia, S. K. (2000). Characterization of pore size distributions of mesoporous materials from adsorption isotherms. *Journal of Physical Chemistry B, 104*(39), 9099–9190. https://doi.org/10.1021/jp000907j

Spada, J. C., Noreña, C. P. Z., Marczak, L. D. F., & Tessaro, I. C. (2013). Water adsorption isotherms of microcapsules with hydrolyzed pinhão (*Araucaria angustifolia* seeds) starch as wall material. *Journal of Food Engineering, 114*(1), 64–69. https://doi.org/10.1016/j.jfoodeng.2012.07.019

Sundaram, J., & Durance, T. D. (2008). Water sorption and physical properties of locust bean gum – pectin – starch composite gel dried using different drying methods. *Food Hydrocolloids, 22*, 1352–1361. https://doi.org/10.1016/j.foodhyd.2007.07.007

Timmermann, E. O. (2003). Multilayer sorption parameters: BET or GAB values? *Colloids and Surfaces A: Physicochemical and Engineering Aspects, 220*(1–3), 235–260. https://doi.org/10.1016/S0927-7757(03)00059-1

Tsami, E., Vagenas, G. K., & Marinos-Kouris, D. (1992). Moisture sorption isotherms of pectins. *Journal of Food Processing and Preservation, 16*(3), 151–161. https://doi.org/10.1111/j.1745-4549.1992.tb00197.x

Vasile, F. E., Judis, M. A., & Mazzobre, M. F. (2020). Moisture sorption properties and glass transition temperature of a non-conventional exudate gum (*Prosopis alba*) from northeast Argentine. *Food Research International, 131*(September 2019), 109033. https://doi.org/10.1016/j.foodres.2020.109033

Velázquez-Gutiérrez, S. K., Figueira, A. C., Rodríguez-Huezo, M. E., Román-Guerrero, A., Carrillo-Navas, H., & Pérez-Alonso, C. (2015). Sorption isotherms, thermodynamic properties and glass transition temperature of mucilage extracted from chia seeds (*Salvia hispanica* L.). *Carbohydrate Polymers, 121*(1), 411–419. https://doi.org/10.1016/j.carbpol.2014.11.068

Viganó, J., Azuara, E., Telis, V. R. N., Beristain, C. I., Jiménez, M., & Telis-Romero, J. (2012). Role of enthalpy and entropy in moisture sorption behavior of pineapple pulp powder produced by different drying methods. *Thermochimica Acta, 528*, 63–71. https://doi.org/10.1016/j.tca.2011.11.011

Xu-Yan, D., Ping-Ping, L., Fang, W., Mu-Lan, J., Ying-Zhong, Z., Guang-Ming, L., Hong, C., & Yuan-Di, Z. (2012). The impact of processing on the profile of volatile compounds in sesame oil. *European Journal of Lipid Science and Technology, 114*(3), 277–286. https://doi.org/10.1002/ejlt.201100059

Zelenka, T. (2016). Adsorption and desorption of nitrogen at 77 K on micro- and mesoporous materials: Study of transport kinetics. *Microporous and Mesoporous Materials, 227*, 202–209. https://doi.org/10.1016/j.micromeso.2016.03.009